

A fluid-inclusion study and genetic model of wolframite-bearing quartz veins, Garganta de los Montes, Spanish Central System

E. QUILEZ, J. SIERRA AND E. VINDEL

Departamento de Cristalografía y Mineralogía, Facultad de C.C. Geológicas, Universidad Complutense, 28040 Madrid, Spain

Abstract

Wolframite-bearing quartz veins from Garganta de los Montes, Madrid province, are hosted by banded gneisses that have undergone intense migmatization processes. The ore deposit is closely related to the La Cabrera granitic batholith. The veins strike 075° and dip 75°S. The mineral association includes wolframite, quartz and minor amounts of scheelite and sulphides (sphalerite, chalcopyrite, pyrrhotite, stannite and marcasite). The fluid phases associated with quartz from the vein margin (early barren quartz) and from the vein centre (late wolframite-bearing quartz) have been studied using microthermometry, scanning electron microscopy and crushing test analyses. Four hydrothermal stages have been distinguished.

The earliest fluids, only recognized in the barren quartz, contain brine, daughter phase (halite) and trapped minerals. The second hydrothermal stage is characterized by complex carbonic–aqueous inclusions of low salinity (3 to 7 wt.% eq. NaCl) and low density (0.4 to 0.7 g.cm⁻³). They mainly homogenize into liquid between 300 and 420°C. The third stage is represented by low to moderate salinity inclusions (<9 wt.% eq. NaCl) of moderate density (0.8 to 0.96 g.cm⁻³), homogenizing between 120° and 330°C. The latest fluids correspond to aqueous solutions of higher salinities (H₂O–NaCl, with Ca²⁺ and Mg²⁺) and densities (>1 g.cm⁻³), with TH ranging between 50 and 130°C. The role of the complex-carbonic aqueous fluids in the transport and precipitation of tungsten is highlighted.

KEYWORDS: fluid inclusions, wolframite, quartz, Spanish Central System.

Geological setting

THE wolframite-bearing quartz veins of Garganta de los Montes are located in the central part of the Spanish Central System, on the northern margin of the La Cabrera granitic batholith. This zone is characterized by the presence of pre-Ordovician lithologies affected by medium- to high-grade regional metamorphism (Fig. 1).

The tungsten deposit is hosted by banded gneisses belonging to the B1 member of the Buitrago Formation (Fernández Casals, 1974) of pelitic provenance, in which layers of quartz, feldspar and cordierite alternate with biotite–sillimanite layers.

The high metamorphic grade to which these rocks were subjected has led to the progressive formation of migmatitic structures. According to descriptive field work, stromatic, ptygmatic, schlieren and nebulitic structures are distinguished. The stromatic structures are charac-

terized by neosomes forming light and dark layers in the paleosome, generally parallel to the plane of schistosity. Ptygmatic structures exhibit highly disharmonic, tortuous folds. The migmatites showing schlieren structures are formed by laminar flow and finally in nebulitic structures paleosome and neosome can no longer be identified separately. Migmatites with pegmatitic facies can be recognized in the deepest zones ('diatexites').

The pluton of La Cabrera constitutes the only granitic outcrop of the area. It corresponds to an evolved granitic intrusion of calc-alkaline trend, composed of granites and granodiorites at the margins (310 ± 14 Ma, 280 ± 5 Ma; Vialette *et al.*, 1981). Numerous aplitic and pegmatitic bands can be recognized in the granite and in the surrounding metamorphic rocks. The last ones introduced tourmaline and muscovite, corresponding to later, more differentiated bodies.

Compared to analyses of 'average' granites,

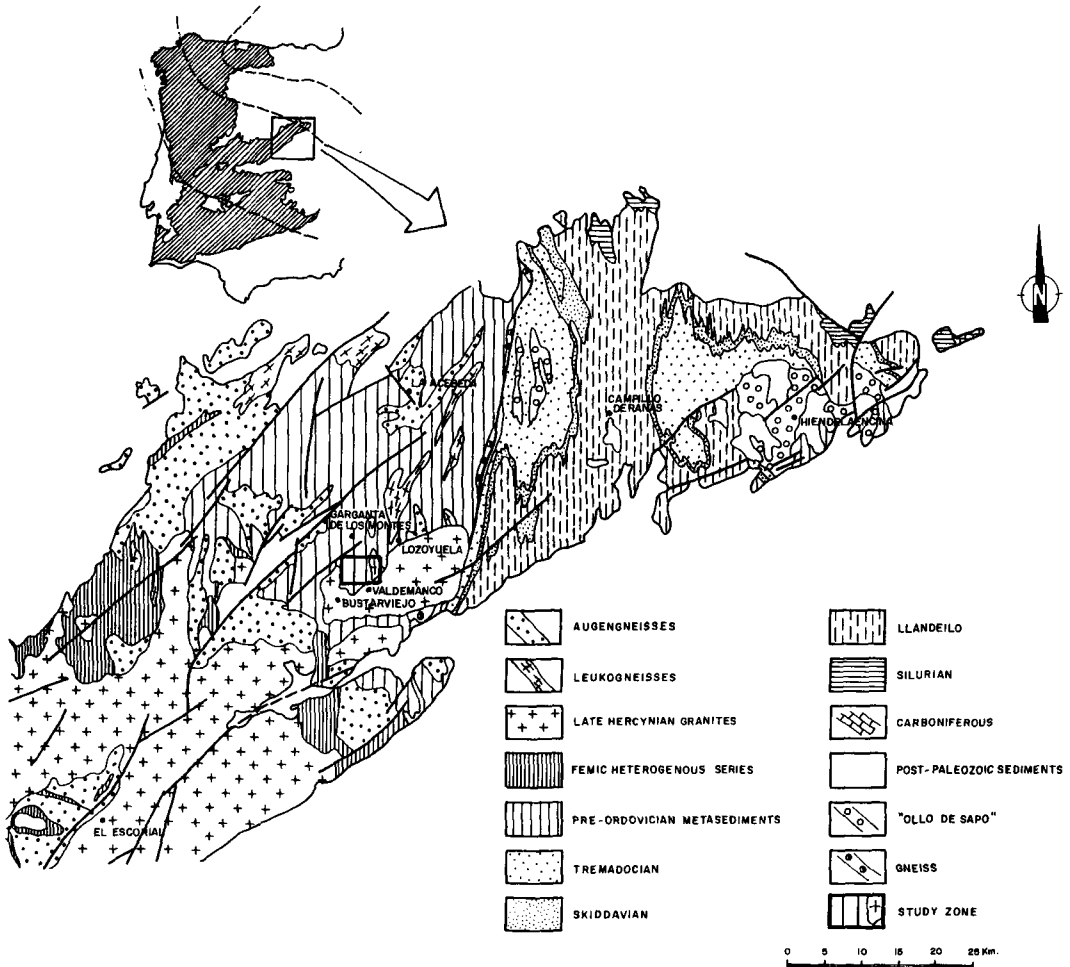


FIG. 1. Geological map of the Spanish Central System, showing study area (Capote *et al.*, 1977).

those of La Cabrera show increased SiO_2 and K_2O contents and lower FeO , MgO , CaO and TiO_2 . Minor element analyses reveal an enrichment in Pb, Rb and Th, with a deficiency of Ba, Ca and Zr (Bellido, 1979). They also contain normative corundum and, therefore, show characteristics of 'specialized granites', spatially and genetically related to Sn-W ore deposits (Tischendorf, 1977).

Tungsten-bearing quartz veins

The ore deposit consists of four main veins striking 075° and dipping 75° southward. The veins vary in width from 1 to 2 m, and show *en echelon* structure in the horizontal direction. Ore was extracted between 1948 and 1955.

The mineral assemblage was first described by Canepa (1968) and later revised by Vindel (1980). The dominant constituent of the veins is massive quartz. Wolframite is concentrated as irregular pods in the vein centre, suggesting that pre-wolframite quartz occurs in the vein margins. Accessory scheelite is the product of alteration of wolframite. Minor amounts of sulphides (sphalerite, chalcopyrite, pyrrhotite, stannite and marcasite) have been found in this study, occurring in cavities and fractures in wolframite and quartz. Covellite, chalcocite and goethite replace primary minerals (Fig. 2).

As a result of the hydrothermal process, alteration affected the wallrocks adjacent to the wolframite-bearing quartz veins. It is difficult to

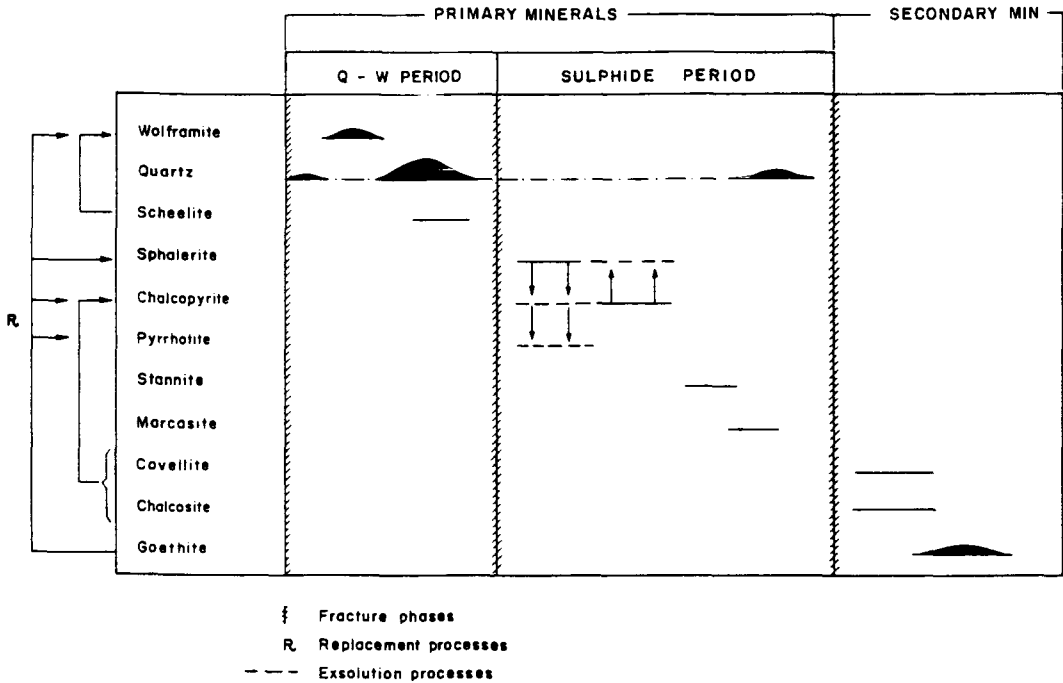


FIG. 2. Mineral paragenesis in the main mineralized stages of the Garganta de los Montes tungsten deposit.

establish the actual spatial distribution of this alteration because granite emplacement induced a wide thermal contact-metamorphic aureole. In spite of this, quartz-sericitization and chloritization are recognized as the most important types of hydrothermal alteration.

Fluid-inclusion study: types of fluid inclusions

In order to define the nature and physicochemical evolution of the mineralizing solutions, fluid inclusions in massive microcrystalline quartz have been studied using microthermometry, crushing test analyses and SEM, with EDS analysis of solid phases.

The quartz samples were collected wherever possible from both the vein margin (V/M) and from the vein centre (V/C), i.e. early barren quartz and later wolframite-bearing quartz respectively. Inclusion sizes range from 5 to 25 μm .

On the basis of their microthermometrically-calculated chemical composition and the phase ratios observed at room temperature, four main types of fluid inclusions have been recognized:

Type I: Inclusions containing brine, daughter phases, and trapped minerals.

Type II: Complex carbonic-aqueous inclusions.

Subtype IIA: Three-phase inclusions at room temperature.

Subtype IIB: Two-phase inclusions at room temperature.

Type III: Low to moderate-salinity aqueous inclusions (H_2O -NaCl).

Type IV: Mixed-salt aqueous inclusions (H_2O -NaCl and other chlorides).





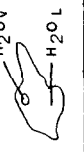
Type I inclusions are present only in the quartz from the vein margin and they are usually isolated. They contain brine, a gas bubble (10–30% of the total inclusion) and one or several solids.

Type II. Two subtypes have been distinguished here. Subtype IIA inclusions are three-phase inclusions at room temperature, containing liquid CO_2 , CO_2 vapour and aqueous phase. They have subrounded shapes and usually occur isolated in the quartz from the vein centre, whereas they are scattered along healed fractures at the margin. These inclusions are the most abundant in the quartz of the Garganta de los Montes deposit.

Subtype IIB are two-phase at room temperature. Vapour occupies between 30 and 70% of the total volume. These fluid inclusions are isolated and extremely abundant at the vein centre, while they occur only rarely in healed fracture planes at the margins.

Type III inclusions are two phase, aqueous and

TABLE 1

MICROTHERMOMETRIC FEATURES	TYPE 1 Solids 	TYPE 2 Subtype 2A 	Subtype 2B 	TYPE 3 	TYPE 4 
SYSTEM	H ₂ O - NaCl	CO ₂ -CH ₄ -NaCl-H ₂ O	H ₂ O-CO ₂ -NaCl	H ₂ O-NaCl	H ₂ O-NaCl-KCl-CaCl ₂ -MgCl ₂
SIZE (μm)	5 to 20	8 to 24	8 to 18	8 to 20	12 to 24
DEGREE OF FILLING	10% to 30%	30% to 70%	30% to 70%	10% to 50%	5% to 10%
T _d disappearance of the vapour phase.	+160 to +340				
T _d decrepitation	+280 to +450				
T _m .CO ₂	-69 to -56				
T _m .Cl.	+6 to +12	+6 to +10			
T _h .CO ₂	+19 to +31				
T _m .ice	-4.6 to -0.2	-6 to -1.8		-5.7 to -0.8	eut: -60 to -40
T _H	+300 to +420	+280 to +350		+120 to +330	+50 to +130
DENSITIES (g/cc)	0.4 to 0.7			0.8 to 0.95	>1
SALINITIES (%eq.wt.NaCl)	3 to 7			1 to 9	15 to 41
THERMOBAROMETRIC CONDITIONS	T>+450°C P>500 bars	T>350°C P>500 bars		T>200°C P>100 bars	T>100°C P>50 bars
OCCURRENCE:	ISOLATED NO	IN FRACTURES ISOLATED	IN FRACTURES ISOLATED	IN FRACTURES IN FRACTURES	IN FRACTURES IN FRACTURES

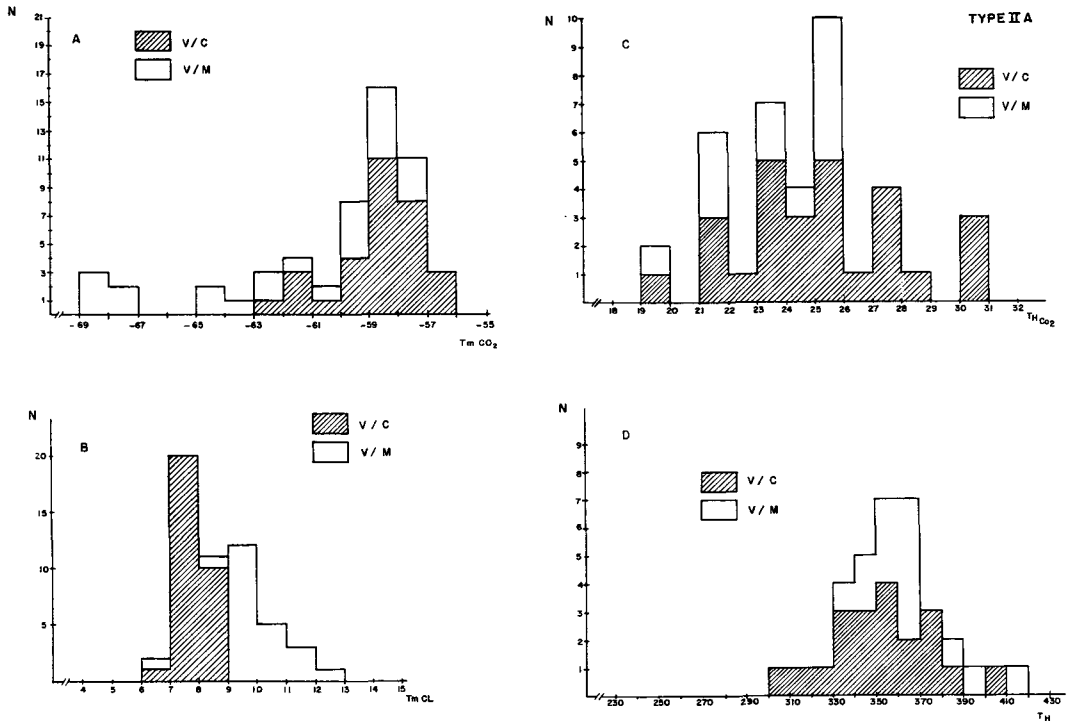


FIG. 3. Microthermometric data of type IIA inclusions. V/C: vein centre V/M: vein margin. A, melting temperature of CO₂ (T_mCO₂); B, melting temperature of clathrate (T_mclath); C, partial homogenization of CO₂ (TH_{CO2}); D, total homogenization (TH) (All in °C).

irregularly shaped, with vapour bubbles amounting to between 10 and 50% of the total volume. They always occur along secondary healed fracture planes in the centre, as well as in the vein margin.

Type IV inclusions are mixed-salt, aqueous, two phase inclusions at room temperature and the volume of the gas bubble comprises 5–10% of the total inclusion. They are scarce in the studied samples and always located in healed fractures.

Microthermometric data

Microthermometric investigations have been performed with a Chaixmecca heating–freezing stage of the type described by Poty *et al.* (1976), using doubly-polished sections of 0.3 mm thickness. Table 1 summarizes the microthermometric features.

Type I inclusions. The disappearance of the vapour phase occurs in the range 160 to 340 °C. However, total homogenization was never achieved due to decrepitation occurring before

the dissolution of the solids. The inclusions decrepitated between 280 and 450 °C. At 450 °C the solids are almost dissolved; consequently this temperature would be near to the total homogenization. This observation indicates that these inclusions probably correspond to the highest-temperature fluids of the deposit.

Sometimes the crystals contained in these inclusions remained unchanged during heating.

Type II. Subtype IIA: the occurrence of CO₂ is indicated by the nucleation of solid CO₂ between –95 and –100 °C during cooling and by the formation of a solid phase considered to be clathrate during the subsequent heating.

The microthermometric data, melting temperatures of CO₂, melting temperatures of clathrate, partial homogenization of CO₂ and total homogenization of the inclusions are displayed in Fig. 3.

The carbonic phase is not pure carbon dioxide as these inclusions exhibit melting temperatures of solid CO₂ between –56.6° (CO₂ triple point) and –69 °C, and occasional clathrate melting temperatures above +10 °C (Hollister and Burruss, 1976; Swanenberg, 1979).

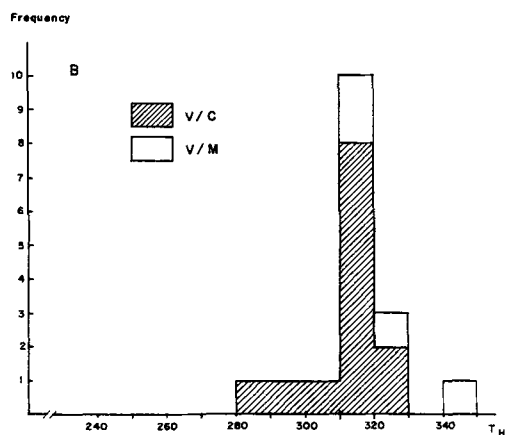
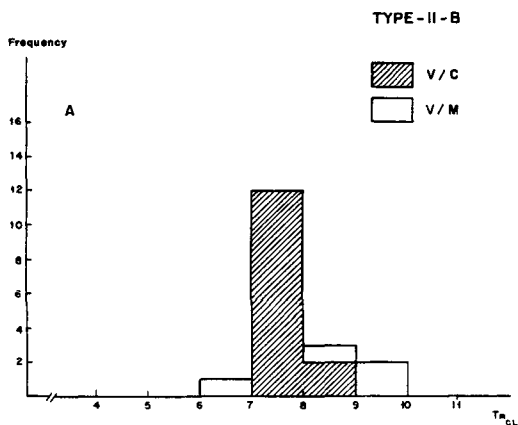


Fig. 4. Type IIB fluid inclusions. A, melting temperature of clathrate ($T_{m,cl}$); B, homogenization temperatures (T_H) (All in $^{\circ}C$).

These inclusions homogenize at temperatures ranging between 300° and 420 $^{\circ}C$, although most of the values are concentrated between 350° and 370 $^{\circ}C$. Homogenization occurs mainly into the liquid phase.

The aqueous phase is a dilute brine with salinities between 3 and 7 wt.% eq. NaCl. The salinities were determined by clathrate melting and by the depression of freezing point due to the effect of dissolved CO_2 in the aqueous phase (Collins, 1979).

The density of the inclusions ranges from 0.4 to 0.75 $g \cdot cm^{-3}$. The calculation is based on the knowledge of the composition and density of the aqueous and carbonic phases at a temperature of <31 $^{\circ}C$.

Subtype IIB: Nucleation of solid CO_2 and for-

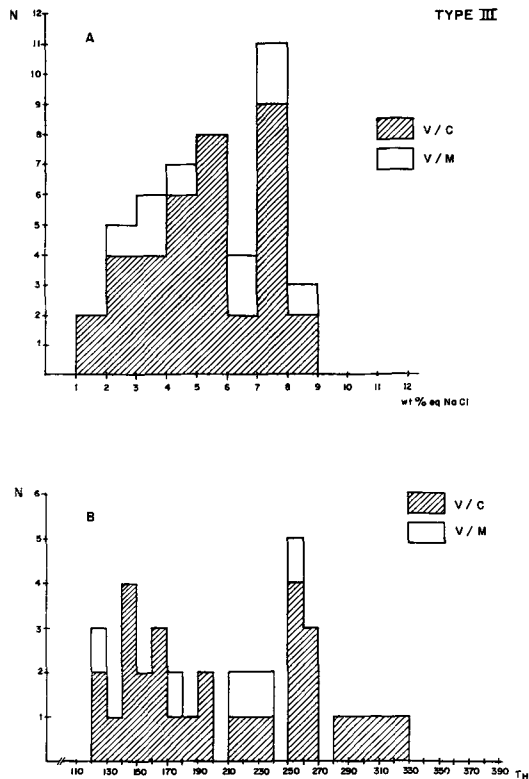


Fig. 5. Type III fluid inclusions. A, salinity expressed in wt.% eq. NaCl; B, homogenization temperatures (T_H) (All in $^{\circ}C$).

mation of liquid CO_2 are not observed in these inclusions. The occurrence of small amounts of carbon dioxide and other volatiles is indicated by the formation, at moderately low temperatures, of a solid phase considered to be clathrate due to its melting temperature of between 6° and 10 $^{\circ}C$ (Fig. 4A).

The fact that liquid CO_2 has never been observed indicates that the amount of CO_2 and volatiles in the fluid phase is small. Homogenization temperatures are between 280° and 350 $^{\circ}C$ (Fig. 4B).

Type III inclusions. This type of inclusion is less abundant than Type II. The temperature of the first observable melting of ice takes place around -20 $^{\circ}C$. These results suggest that the aqueous solution contains mainly Na^+ cations in solution. The final melting temperature of ice values range between -0.8° to -5.7 $^{\circ}C$, indicating a salinity lower than 9 wt.% eq. NaCl, with most between 7 and 8 wt.% eq. NaCl (Fig. 5A).

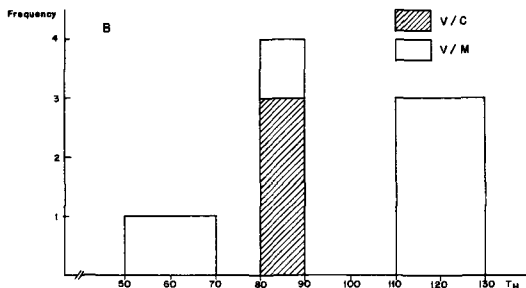
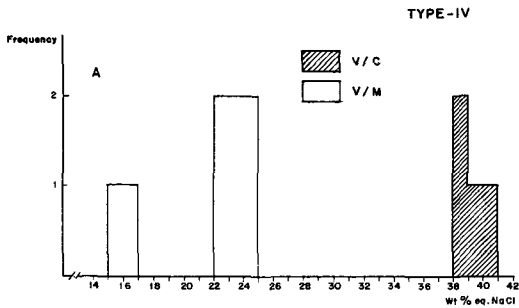


Fig. 6. Type IV fluid inclusions. A, approximate salinity expressed in wt.% eq. NaCl; B, homogenization temperatures (TH) (°C).

Homogenization temperatures are widely scattered between 120° and 330°C (Fig. 5B). All inclusions homogenize into the liquid phase.

Densities for these inclusions (0.8 to 0.96 g.cm⁻³) were calculated using the homogenization temperatures and salinities of Ahmad and Rose, 1980.

Type IV inclusions. On cooling, these inclusions exhibit special characteristics: the ice begins to melt between -40° and -60°C, and the final melting temperature of ice ranges from -22.3° to -11.7°C.

In accordance with the eutectic temperatures and the final temperatures of ice-melting, it is likely that the trapped solution contains significant amounts of CaCl₂ or MgCl₂ (Crawford, 1981). The approximate value of the salinity in terms of the final melting temperature of ice is over 15 wt.% eq. NaCl (Fig. 6A).

During heating, these inclusions homogenize into the liquid phase between 50° and 130°C (Fig. 6B). The calculated density is greater than 1 g.cm (Ahmad and Rose, 1980).

Electron microscope data

Qualitative analysis of the solid phases contained in the Type I inclusions was undertaken by electron microscopy with coupled energy-dispersive detectors. The determinations were performed combining the morphology of the solids with qualitative chemical analysis. Solid phases found in the cavities are halite cubes (as a daughter mineral) and lamellar muscovite (probably a trapped mineral).

Crushing tests

The crushing-test analyses were carried out using a Chaixmecca crushing stage. The experiments were carried out on 8 samples: 5 on wolframite-bearing quartz from the vein centre (V/C) and vein margin (V/ME, V/MW, V2/MW, V3/ME), 1 on wolframite (V/C), 1 on the barren quartz vein and 1 on the pegmatite. Between 5 and 10 crushing tests were performed on every sample. The liberated gas intensity was evaluated using the crushing test of Leroy (1979).

Histograms of crushing-test analyses (Fig. 7) exhibit the following characteristics:

- (1) The liberated gas intensity from the quartz of the vein centre (V/C) was strong (Fig. 7a), whereas that from the quartz of the vein margin (V/ME, V/MW, V2/MW, V3/ME) was intermediate (Fig. 7b, c, d and e).
- (2) Wolframite shows very strong liberated gas intensity (Fig. 7f).
- (3) The barren quartz vein and pegmatite also show strong liberated gas intensity (Fig. 7g and h).

The data above indicate that fluids trapped throughout the vein complex contain considerable quantities of gaseous carbonic compounds. These results agree with the microthermometric analyses, thus indicating that the liberated gas intensity decreases from the centre towards the vein margin. The presence of those gases in wolframite suggests some relation between this mineral and the CO₂-aqueous fluids. The important amount of gas liberated by the pegmatite indicates the relevance of carbonic vapours in the last stage of the granite evolution.

Hydrothermal evolution of the Garganta de los Montes deposit

Estimation of the fluids' thermobarometric conditions was made on the basis of the microthermometric data and experimental data calculated for the systems H₂O (Fisher, 1976), H₂O-NaCl (Potter and Brown, 1977) and H₂O-CO₂-NaCl

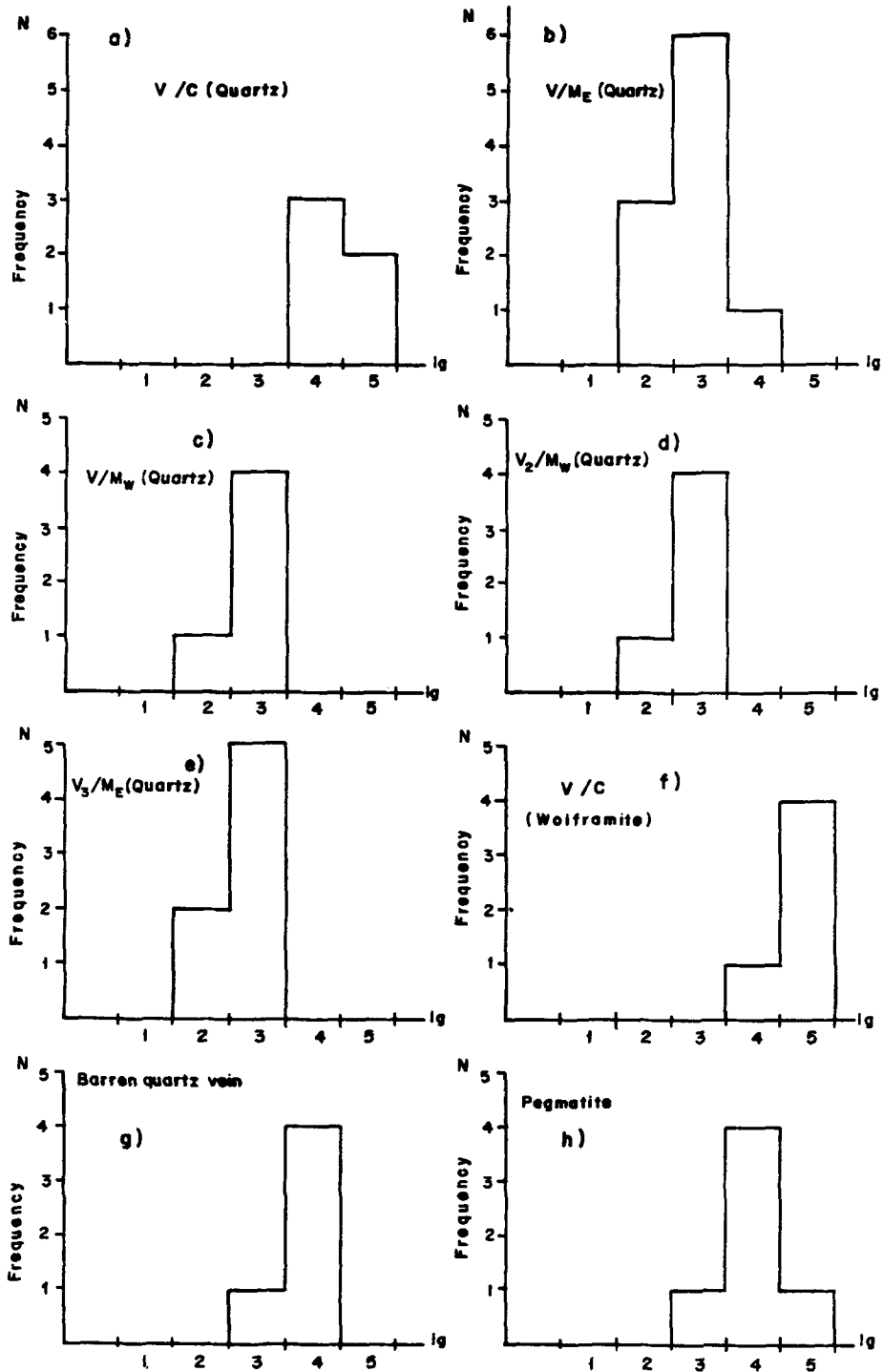


Fig. 7. Results of crushing-test analyses. N, number of analyses; Ig, intensity of liberated gas using the crushing test of Leroy (1979); V/C, vein centre; V/ME, vein east margin; V/MW, vein west margin; V₂/MW, associated vein west margin; V₃/ME, associated vein east margin.

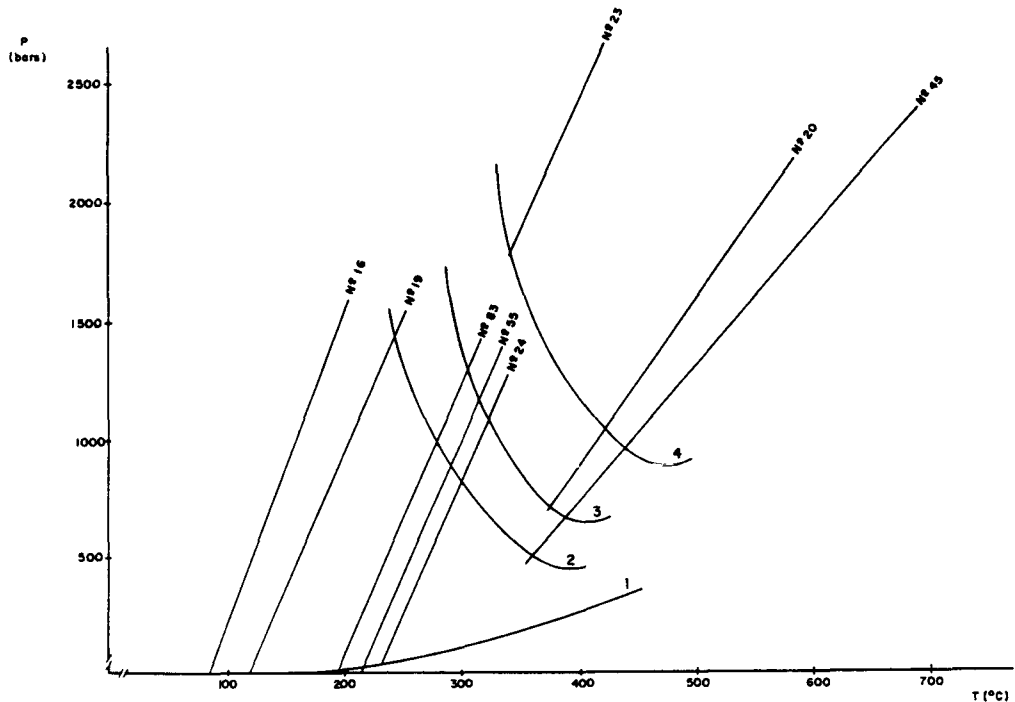


FIG. 8. P - T diagram exhibiting significant isochores of Type II (Nos. 20, 23, 45), Type III (Nos. 24, 55, 83) and Type IV (Nos. 16 and 19) inclusions. Isocompositional curves: 1, (H_2O); 2, (7 mol.% CO_2 , 4 wt.% NaCl); 3, (10 mol.% CO_2 , 5 wt.% NaCl); and 4, (21 mol.% CO_2 , 5 wt.% NaCl).

(Gherig, 1980). Since there are no data for the system H_2O -NaCl- CO_2 - CH_4 some selected isochores of representative inclusions were constructed using a modified Redlich-Kwong equation with the Nicolls and Crawford (1985) computer program. The isochores of representative H_2O -NaCl inclusions were calculated using the Potter and Brown (1977) tables. The isochores were then projected into the isocompositional curves on P - T diagrams (Fig. 8).

Based on the results obtained in this study four hydrothermal stages have been defined:

(1) *The first hydrothermal stage* probably corresponds to an early high temperature fluid, is represented by trapping of Type I inclusion containing brine and halite as daughter minerals.

(2) *The second hydrothermal stage* is characterized by complex carbonic-aqueous solutions (Type II inclusions) circulating at minimum temperatures in the range of 300° to 420 °C, and pressures above 500 bars.

(3) *The third hydrothermal stage* corresponds to the circulation and trapping of low to moderate salinity aqueous solutions, represented by Type III inclusions, homogenizing at low to moderate

temperatures (120–330 °C) and pressures above 100 bars.

(4) *The final stage*: the hydrothermal evolution ended with cooler fluids, corresponding to aqueous solutions of higher salinities (H_2O -NaCl with Ca^{2+} and/or Mg^{2+}) at minimum trapping temperatures below 130 °C and pressures above 50 bars.

Therefore, the hydrothermal evolution of the Garganta de los Montes tungsten deposit results from several stages of fluid generation, with decreasing temperatures and pressures. An homogenization temperature-density diagram (Fig. 9) indicates that with descending temperature the solutions increase in density and contain decreasing amounts of CO_2 and volatile compounds. The dilution of the complex CO_2 -aqueous fluid is represented by the trapping of subtype IIB inclusions.

Discussion and conclusions

The fluid inclusion study at the Garganta de los Montes ore deposit provides a better understanding of the circulation of hydrothermal solu-

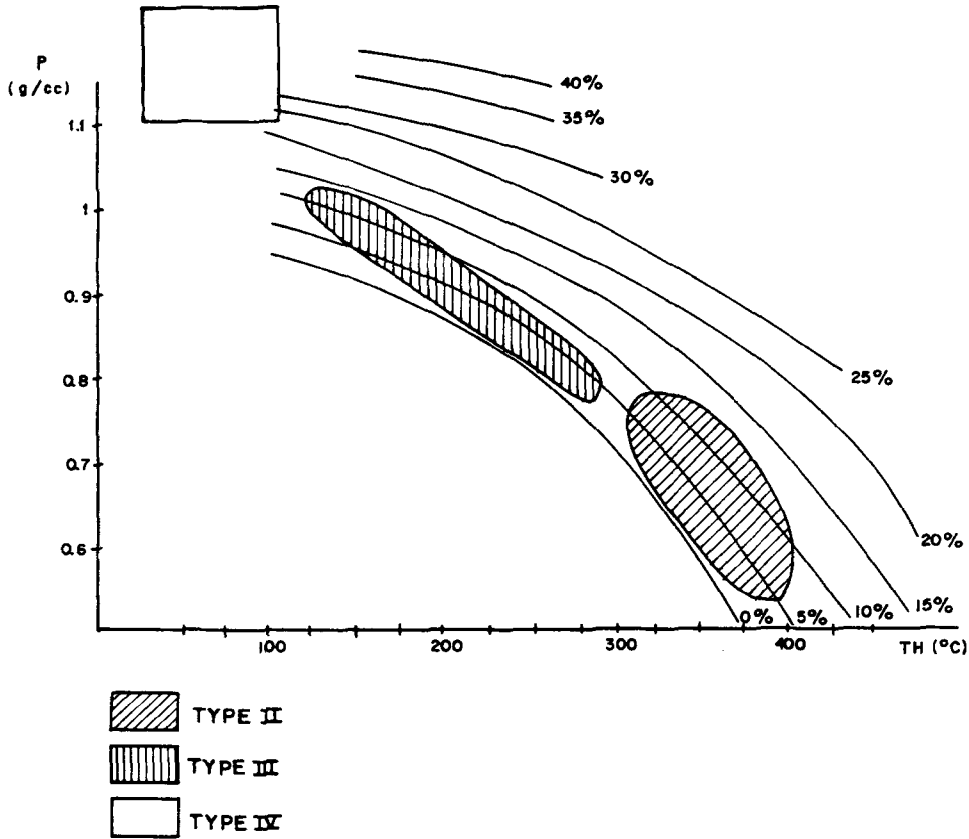


Fig. 9. Homogenization temperature–density diagram of fluid inclusions in quartz from Garganta de los Montes, showing the hydrothermal evolution (0–40% lines indicate salinity).

tions, most probably of magmatic origin. Early brine high-temperature fluids have probably circulated during a first phase of faulting. They were trapped as Type I inclusions in early barren quartz that, after a second stage of fracturing, remained at the vein margins. No brine inclusions have been observed in the vein centre. Similar saline solution are described in the scheelite-bearing quartz vein from Poblet (Catalonian Coastal Range, Spain; Ayora *et al.*, 1987), as well as in the Sn–W deposit of Aouam (Morocco; Cheilletz, 1984).

Later, complex carbonic–aqueous solutions circulated from 300° up to 420°C and pressures of up to 0.5 kbar, and were associated with the wolframite-bearing quartz of the vein centre. Type II inclusions are encountered isolated in the quartz of the vein centre and in healed fractures at the margins. These remarks suggest that complex carbonic–aqueous fluids may play an important role in the transport of tungsten. This conclusion has been proposed in experimental

works (Ivanova *et al.*, 1976; Higgins, 1980) and for other W–Sn deposits (Ball *et al.*, 1985; Shepherd *et al.*, 1985). The predominance of HCO_3^- and CO_2 in these fluids suggests that carbonate and bicarbonate complexes may be responsible for tungsten transport (Higgins, 1980).

Regarding possible genetic links between two fluids, no intermediate compositions have been observed between Type I and Type II. Accordingly, one may suppose that the two fluids belong to two distinct hydrothermal episodes. This conclusion is in agreement with the early character of the brine inclusions and the later trapping of the Type II inclusions.

Subsequently a new phase of fracturing allowed the flow of cooler, low to moderate salinity (1–9 wt.% eq. NaCl) aqueous fluids, which may be related to the sulphides accompanying wolframite. Temperatures of between 120° and 330°C, and pressures of 100 bar are minimum estimates of temperature and pressure at the time of trap-

ping. Towards the end of the hydrothermal evolution, the salinity of the fluids increased greatly, as shown by type IV inclusions which homogenize below 130°C.

Taking into account that the wallrock adjacent to the wolframite-bearing veins has undergone intense hydrothermal alteration, the wolframite precipitation could have been favoured by fluid-rock interaction. The reaction with the host rocks caused progressive cooling of the solutions and increased the fluid pH by loss of H⁺ used in the sericitization of feldspar and chloritization of biotites, thus destabilizing the tungsten-bearing complexes. On the other hand, the carbonic vapour dilution by cooler aqueous fluids may be also a mechanism that favoured the precipitation of the tungsten.

Finally, a similar hydrothermal evolution has been proposed for other Spanish W-Sn ore deposits, e.g. La Parrilla, La Fregeneda, Golpejas, Laza, Teba, and San Finx (Mangas, 1987a, b, 1988); however, Type I brine inclusions have not been recognized in them.

References

- Ahmad, S. N. and Rose, A. W. (1980) Fluid inclusions in porphyry and skarn ore at Santa Rita, New Mexico. *Econ. Geol.* **75**, 229–50.
- Ayora, C., Guilhaumou, N., Touray, J. C. and Melgarejo, J. C. (1987) Scheelite-bearing quartz veins from Poblet (Catalonian Coastal Range). Characterization of fluid inclusions and genetic model. *Bull. Mineral.* **110**, 603–11.
- Ball, T. K., Fortey, N. J. and Shepherd, T. J. (1985) Mineralization at the Carrock Fell Mine, Cumbria, Northern England. *Mineral Deposita*, **20**, 57–65.
- Bellido, F. (1979) *Estudio petrológico y geoquímico del plutón granítico de La Cabrera (Madrid)*. Ph.D. thesis, Univ. Complutense, Madrid.
- Canepa, C. (1968) *Contribución a la metalogenia de la Sierra de Guadarrama (Hojas 484 y 509, Provincia de Madrid)*. Ph.D. thesis, Univ. Complutense, Madrid.
- Capote, R., Casquet, C., Fernandez Casals, M. J., Moreno, F., Navidad, M., Peinado, M. and Vegas, R. (1977) The Precambrian in the central part of the Iberian massif. *Estudios Geol.* **33**, 343–55.
- Cheilletz, A. (1984) Caractéristiques géochimiques et Thermobarométriques des fluides associés à la sheelite et au quartz des mineralisations de Tungstène du djebel Aoun (Maroc. Central). *Bull. Mineral.* **107**, 255–72.
- Collins, P. L. F. (1979) Gas hydrates in CO₂-bearing fluid inclusions and the use of freezing data for estimation of salinity. *Econ. Geol.* **74**, 1435–44.
- Crawford, M. L. (1981) Phase equilibria in aqueous fluid inclusions. In *Short course in fluid inclusions: applications to petrology*. (L. S. Hollister and M. L. Crawford, eds.), 75–100.
- Fernández Casals, M. J. (1974) Significado geotectónico de la formación Gneises de la Morcuera. *Studia Geologica*, **7**, 87–106.
- Fisher, J. R. (1976) The volumetric properties of H₂O: a graphical portrayal. *J. Research U.S. Geol. Survey*, **4**, 189–93.
- Gherig, M. (1980) *Phasenpleichgewichte und PVT daten ternarer mischungen aus wasser kohlendioxid und natriumchlorid bis 3KD und 550°C*. Ph.D. Thesis, Karlsruhe.
- Higgins, N. C. (1980) Fluid inclusion evidence for the transport of tungsten by carbonate complexes in hydrothermal solutions. *Can. J. Earth. Sci.* **17**, 823–30.
- Hollister, L. S. and Burruss, R. C. (1976) Phase equilibria in fluid inclusions from the Khtada Lake metamorphic complex. *Geochim. Cosmochim. Acta*, **40**, 163–75.
- Ivanova, G. F., Khitarov, D. N., Levkina, N. I., Milvsky, G. A. and Bannykh, L. P. (1976) Gas-liquid inclusion data on the composition of Tungsten bearing hydrothermal solutions. *Geochem. Internat.* **13**, 17–26.
- Leroy, J. (1979) Contribution é l'étalonnage de la pression interne des inclusions fluids lors de leur décrépiation. *Bull. Soc. Fr. Mineral. Cristallogr.* **102**, 584–93.
- Mangas, J. (1987a) *Estudio de las inclusiones fluidas en los yacimientos españoles de estaño asociados a granitos hercínicos*. Ph.D. thesis, Univ. Salamanca.
- (1987b) Fluid inclusion study on different types of tin deposits associated with the Hercynian granites of Western Spain. *Chem. Geol.* **61**, 193–208.
- (1988) Hydrothermal fluid evolution of the Sn-W mineralization in the Parrilla ore deposit (Caceres, Spain). *J. Geol. Soc. London*, **145**, 147–55.
- Nicolls, J. and Crawford, M. L. (1985) Fortran programs for calculation of fluids properties from microthermometric data on fluid inclusions. *Computers and Geosciences*, **11**, 619–45.
- Potter, R. W. and Brown, D. L. (1977) The volumetric properties of aqueous sodium chloride solutions from 0° to 500°C and pressures up to 2000 bars based on a regression of available data in the literature. *U.S. Geol. Survey Bull.* 1421-C.
- Poty, B., Leroy, J. and Jachimowicz, L. (1976) Un nouvel appareil pur las mesure des températures sous le microscope: l'installations de microthermométrie Chaixmeca. *Bull. Soc. Fr. Mineral. Cristallogr.* **99**, 182–7.
- Shepherd, T. J., Miller, M. F., Scrivener, R. C. and Darbyshire, D. P. F. D. (1985) Hydrothermal fluid evolution in relation to mineralization in southwest England with special reference to the Dartmoor-Bodmin area. In *High heat producing (HHP) granites, hydrothermal circulation and ore genesis*. Inst. Mining Metall., 345–64.
- Swanenberg, H. E. C. (1979) Phase equilibria in carbonic systems, and their application to freezing studies of fluid inclusions. *Contrib. Mineral. Petrol.* **68**, 303–6.
- Tischendorf, G. (1977) Geochemical and petrographic

- characteristic of silicic magmatic rocks associated with rare element mineralization. In *Metallization associated with Acid Magmatism*. (M. Stempok, L. Burnol and G. Tischendorf, eds.), 2, 41–96.
- Vialette, Y., Bellido, F., Fuster, J. M. and Ibarrola, E. (1981) Données géochronologiques sur les granites de la Cabrera. *Cuadernos de Geología Ibérica*, 7, 327–35
- Vindel, E. (1980) *Estudio mineralógico y petrológico de las mineralizaciones de la Sierra del Guadarrama*. Ph.D. thesis, Univ. Complutense, Madrid.

[Manuscript received 5 April 1989;
revised 2 February 1990]